Hydrological Sciences—Journal—des Sciences Hydrologiques, **43**(4) August 1998
Special issue: *Monitoring and Modelling of Soil Moisture: Integration over Time and Space*

Kinematic wave approach to drainage flow and moisture distribution in a structured soil

A. MDAGHRI-ALAOUI & PETER F. GERMANN

Soil Science Section, Institute of Geography, University of Berne, Hallerstrasse 12, CH-3012 Berne, Switzerland

e-mail: PGERMANN@giub.unibe.ch

Abstract Infiltration experiments with intensities varying from 4.1×10^{-6} to 2.8×10^{-5} m s^{-1} were conducted on a column of undisturbed soil. Flow was investigated using kinematic wave theory. The approach was first applied to the drainage curve of outflow. In this case, preferential flow occurred during intermediate infiltration rates. The approach was further applied to soil moisture variations at three depths of the column. The wetting front dispersion increased with depth according to the analysis of mobile soil moisture contributing to total flow, whereas the analysis of mobile soil moisture contributing to rapid flow indicated flow through macropores. The kinematic wave model simulates reasonably well both measured drainage of outflow and of soil moisture. A simple method was used to separate mobile soil moisture contributing to rapid flow and that contributing to diffusive flow. The validity of the model was evaluated by water balance comparison, with particular attention given to the distinction between the two types of soil moisture.

Application de l'approche de l'onde cinématique sur le flux de drainage et la distribution de l'humidité dans un sol structuré

Résumé Des essais d'infiltration d'intensité variant entre 4.1×10^{-6} et 2.8×10^{-5} m s^{-1} ont été effectués sur une colonne de sol non remanié. L'écoulement a été étudié en s'appuyant sur la théorie de l'onde cinématique. Cette théorie a d'abord été appliquée à la courbe du flux de drainage. Dans ce cas, le flux préférentiel a lieu durant les pluies à intensité intermédiaire. L'approche a ensuite été appliquée aux courbes représentant les variations de la teneur en eau à différentes profondeurs de la colonne. L'analyse de la courbe de la teneur en eau mobile contribuant à l'écoulement total met en évidence la dispersion du front d'humectation avec la profondeur. Par ailleurs, l'analyse des courbes de teneur en eau mobile contribuant à l'écoulement rapide indique un écoulement dans les macropores. Les courbes du flux de drainage et de la teneur en eau ont été raisonnablement reproduites par la théorie de l'onde cinématique. Une méthode simple a été utilisée pour séparer les deux types de teneur en eau mobile. La crédibilité de cette méthode a été évaluée par le bilan hydrique.

INTRODUCTION

Water flowing in macropores may bypass much of the water stored in the finer pores (Smettem & Trudgill, 1983; Booltink & Bouma, 1991) resulting in the appearance of "new" input water at considerable depth, with comparatively little mixing or displacement of the previously stored ("old") soil water (Leaney *et al.*, 1993).

Various approaches to bypass flow consider the soil matrix–macropore dichotomy. Macropores not only dominate the infiltration of ponded water (Smettem &

Collis-George, 1985) but also play a major role during flux-infiltration after matrix ponding has occurred (Clothier & Heiler, 1983). From this perspective, Jarvis (1994) developed a physically-based model of water and solute transport in macroporous soil. The model divides the total soil porosity into two components, macropores and micropores, and may be run in either one or two flow domains. Chen & Wagenet (1992) simulated water and chemical transport by combining the Richards (1931) equation for transport in the soil domain with the Hagen-Poiseuille and Chezy-Manning equations for macropore transport. Germann & Beven (1985) and Germann (1990) applied kinematic wave theory to bypass flow. They modelled the infiltration and drainage of square pulses in the macropore continuum. Recently, kinematic wave theory was applied to temporal soil moisture variations during infiltration into the unsaturated zone (Mdaghri-Alaoui, 1995; Germann & Bürgi, 1996).

In this study, kinematic wave theory was applied to drainage flow and the temporal variation of soil moisture at three depths during and shortly after the infiltration of various pulses of water into a column of undisturbed soil. The coherent applicability of the kinematic wave approach to both soil moisture and outflow supports the notion that the model parameters indicate whether water flows predominantly through the matrix or through macropores. The principal aims of this study are: (a) to investigate the outflow and soil moisture, and (b) to estimate the limit between mobile soil moisture contributing to rapid flow and mobile soil moisture contributing to diffusive flow, according to the kinematic wave theory. The validity of the model, particularly with respect to the distinction between the two types of soil moisture, is evaluated by water balance comparison.

THEORY

Flow occurs along the steepest energy gradient. In soil–water systems energy transfer is due to either maximizing the curvature of the menisci or viscosity. Maximization of the water surface curvature leads to the diffusion of capillary potential, as expressed by the Richards equation (Germann & Di Pietro, 1996).

Dingman (1984) views kinematic viscosity ($L^2\ T^{-1}$) as the coefficient of dissipation of momentum due to viscosity as expressed by boundary-layer flow theory. The kinematic viscosity of water is approximately 10^{-6} $m^2\ s^{-1}$. Germann *et al.* (1997) argued that energy dissipation has to be considered to occur concurrently with the diffusion of capillary potential whenever the capillary diffusivity is greater than the kinematic viscosity. From a fluid dynamics point of view, local gradients at the scale of pores or water laminae will govern energy transfer due to either capillarity or viscosity. This leads to mixed behaviours at the fluid mechanics scale. Moreover, the length scales of the two modes of energy transfer cannot *a priori* be assumed to be equal, thus leading to the phenomenon of preferential flow. The theory of kinematic waves can be applied to the dissipation of momentum during porous media flow, and the method of characteristics deals with the moving boundary (Germann, 1990). In the following, mobile soil moisture contributing to total flow and the fraction contributing to rapid flow are abbreviated by θ and w (both in $m^3\ m^{-3}$), respectively.

The separation of the two types of soil moisture is experimental and will be based on the parameters of the kinematic wave model applied to specific sets of data.

Germann (1990) derived the following relation from boundary-layer flow theory:

$$q = bw^a \tag{1}$$

where q (m s^{-1}) is the volume flux density, w (m^3 m^{-3}) is the mobile moisture content, b (m s^{-1}) is the conductance and a is a dimensionless exponent. The following balance equation applies:

$$\frac{\partial q}{\partial t} + c\frac{\partial q}{\partial z} = 0 \tag{2}$$

where the celerity c (m s^{-1}) (the one-dimensional propagation velocity of a water property) is defined as:

$$c = \frac{\mathrm{d}q}{\mathrm{d}w} = \left.\frac{\mathrm{d}z}{\mathrm{d}w}\right|_{q,w} = abw^{(a-1)} = ab^{1/a}q^{(a-1)/a} \tag{3}$$

The initial and boundary conditions are:

$$\begin{aligned} &t \le 0, && t \ge t_s, && q(0,t) = w(0,t) = 0 \\ &0 \le t \le t_s && q(0,t) = q_s && w(0,t) = w_s = \left(\frac{q_s}{b}\right)^{1/a} \\ &0 \le z \le \infty && q(z,0) = w(z,0) = 0 \end{aligned} \tag{4}$$

At $t = 0$, a wetting front starts moving as a kinematic shock wave with celerity:

$$c_W = \frac{q_s}{w_s} = \frac{\partial z_W}{\partial t} = bw_s^{(a-1)} = b^{1/a}q_s^{(a-1)/a} = \frac{\partial z_W(t)}{\partial t} \tag{5a}$$

The separation of variables and integration leads to the position $z_W(t)$ (m) of the wetting front:

$$z_W(t) = tbw_s^{(a-1)} = tb^{1/a}q_s^{(a-1)/a} \tag{5b}$$

Conversely, the time lapsed for the wetting front to move to depth z is:

$$t_W(z) = \frac{z}{bw^{(a-1)}} = \frac{z}{b^{1/a}q_s^{(a-1)/a}} \tag{5c}$$

A draining front (indexed D) is released at the soil surface at the end of infiltration at $t = t_s$ with celerity:

$$c_D = \frac{\partial z_D}{\partial t} = abw_s^{(a-1)} = ab^{1/a}q_s^{(a-1)/a} = \frac{\partial q}{\partial w} \tag{6a}$$

Following similar procedures to those above leads to the position of the draining front:

$$z_D(t) = (t - t_s)abw_s^{(a-1)} = (t - t_s)ab^{1/a}q_s^{(a-1)/a} \tag{6b}$$

and the time lapsed to move to z:

$$t_D(z) = t_s + \frac{z}{abw_s^{(a-1)}} = t_s + \frac{z}{ab^{1/a}q_s^{(a-1)/a}} \tag{6c}$$

Equations (5b), (5c) and (6b), (6c) are the characteristics of the wetting and draining fronts, respectively. They permit the solution of the partial differential equation (equation (2)) with a set of ordinary differential equations.

From equations (5a) and (6a) it follows that:

$$a = \frac{c_D}{c_W} = \frac{t_W(Z)}{t_D(Z) - t_s} \tag{7}$$

where Z (m) $\leq z_I$. Because $c_D = a \times c_W$, the draining front will intercept the wetting front at time

$$t_I = \frac{t_s a}{(a-1)} \tag{8a}$$

The corresponding depth is

$$z_I = t_s \frac{a}{(a-1)} bw_s^{(a-1)} = t_s \frac{a}{(a-1)} b^{1/a} q_s^{(a-1)/a} \tag{8b}$$

Mobile soil moisture and the volume flux densities of a kinematic wave in the section of $0 \leq z \leq z_I$ are:

$$0 \leq t \leq t_W(z), \qquad w(z,t) = 0 \tag{9a}$$

$$q(z,t) = 0 \tag{9b}$$

$$t_W(z) \leq t \leq t_D(z)\,, \; w(z,t) = w_s \tag{10a}$$

$$q(z,t) = q_s \tag{10b}$$

The mobile soil moisture of the trailing wave for $0 \leq z \leq z_D$ and $t_s \leq t < \infty$ is:

$$w(z,t) = \left[\frac{z}{(t-t_s)ab}\right]^{1/(a-1)} \tag{11a}$$

and

$$q(z,t) = \left[\frac{z}{(t-t_s)ab^{1/a}}\right]^{a/(a-1)} \tag{11b}$$

The mobile soil moisture of the trailing wave and its corresponding volume flux density vary in the range of $0 \leq w(z, t) \leq w_s$ and $0 \leq q(z, t) \leq q_s$, respectively.

The combination of equations (6c) and (11) leads to the trailing wave at depth $z_D(t)$:

$$w(z,t) = w_s \left\{ \frac{t_D(z) - t_s}{t - t_s} \right\}^{1/(a-1)} \tag{12a}$$

$$q(z,t) = \left\{ \frac{z}{(t - t_s) a b^{1/a}} \right\}^{a/(a-1)} \tag{12b}$$

From which follows that

$$a = \frac{(U+1)}{U} \quad \text{with} \quad U = \frac{\left[\ln w(z,t) - \ln w_s\right]}{\ln\left[t_D(z) - t_s\right] - \ln\left[t - t_s\right]} \tag{13a}$$

or

$$a = \frac{V}{(V-1)} \quad \text{with} \quad V = \frac{\left[\ln q(z,t) - \ln q_s\right]}{\ln\left[t_D(z) - t_s\right] - \ln\left[t - t_s\right]} \tag{13b}$$

Equation (13a) or (13b) can be used to estimate exponent a from measurements during $t \geq t_D(Z)$ if $t_D(Z)$ is known.

From the application of equations (5c) and (6c) it follows that:

$$b = \frac{w_s^{(1-a)} Z}{a\left[t_D(Z) - t_s\right]} = \frac{w_s^{(1-a)} Z}{t_W(Z)} \tag{14}$$

The computation of the momentum balance at depth Z (at which the water content is measured) requires the water balance. Thus the total volume of water flowing across the section at depth Z is obtained by integrating the function $w(z, t)$ (equations (10a) and (12a)) with respect to equation (1):

$$V(Z) = b w_s^a \left[\int_{t_W}^{t_D} \mathrm{d}t + \left(t_D - t_s\right)^{a/(a-1)} \int_{t_D}^{\infty} \left(t - t_s\right)^{-a/(a-1)} \mathrm{d}t \right] \tag{15}$$

which, after integration, results in (Germann *et al.*, 1997):

$$V(Z) = b w_s^a \left[a t_D - t_W - (a-1) t_s \right] = b w_s^a(Z) \cdot t_s = q_s(Z) \cdot t_s \tag{16}$$

MATERIAL AND METHODS

The soil originated from calcareous silty-sandy lake sediments from the Ile de St Pierre in the lake of Bienne (Switzerland). It has formed in the last 120 years after the lake level had been lowered by several metres. The horizon 0–0.16 m is well structured with a porosity of 0.52. The porosity is 0.50 in the lower part of the profile below 0.16 m, pH is 7 throughout. The bulk density increases slightly with depth. The texture is sandy loam in the topsoil, and sand in the subsoil.

The untilled soil is a fluvisol characterized by a well-aggregated A_h-horizon

(0–0.05 m). The vegetation was perennial and consisted of herbs (non-abundant) and grasses which measured about 5 cm during the experiments. Networks of macropores, root channels and earthworm burrows to 0.70–0.80 m depth revealed high biological activity. The B-horizon depth (0.15–0.45 m) comprised a loamy sand/sand. The C-horizon below 0.45 m consisted of sand.

A column of undisturbed soil 0.39 m in diameter and 0.43 m long was prepared by driving a bevelled stainless steel cylinder into the ground while continuously removing the surrounding soil material. The undisturbed soil core was then transported to the laboratory in a plastic bag placed in a cushioned container to minimize evaporation and compaction.

The experimental laboratory set up is shown in Fig. 1. Irrigation was supplied by a rainfall simulator consisting of a metallic disc perforated with 72 holes connected to small tubes. Precipitation intensity and duration were controlled by a pump. Soil water content at depths of 0.12, 0.26 and 0.33 m was measured by time domain reflectrometry (TDR, Tektronix 1502B cable tester). The probes consisted of a pair of rods, 6 mm in diameter and 0.25 m long. They were inserted horizontally into the column. Calibration was according to Roth *et al.* (1990). The matrix potential was measured with three tensiometers at depths of 0.12, 0.26 and 0.40 m. Tensiometers

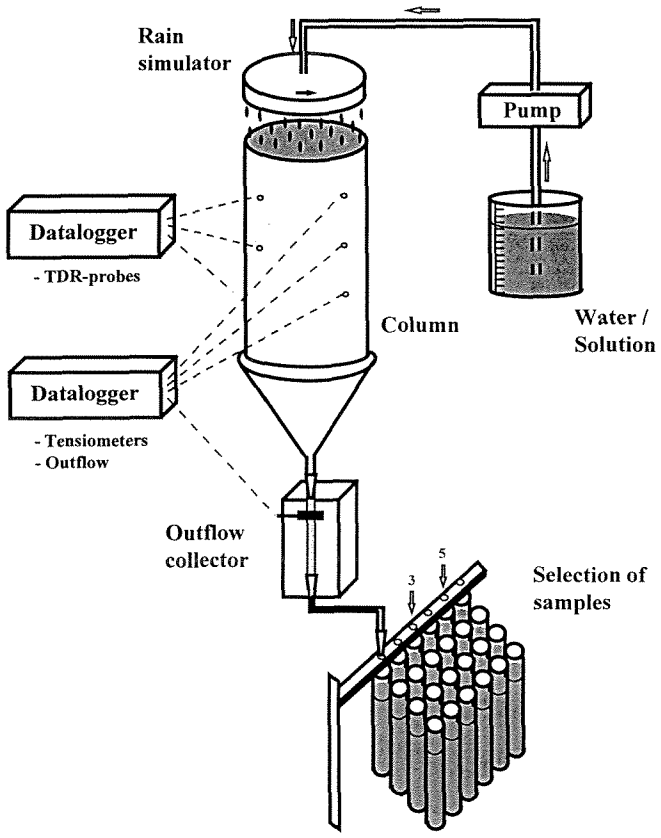

Fig. 1 Experimental setup.

should be sufficiently large to represent hydraulic soil conditions adequately and thus those used were 5 cm long with a diameter of 0.6 cm. To prevent erosion of the column, a disk perforated with square holes (the dimension of each hole is 7 × 7 cm) was placed at the bottom.

The soil column was placed on a funnel connected to an outflow collector. The parameters were measured automatically by a data-logger. In this study, six successive infiltrations of increasing intensities were conducted on the soil column (Table 1). Steady state conditions were established for all infiltrations. The time interval of the measurements, Δt, was 300 s. No application exceeded the soil infiltration rate as no ponding was observed. Visual observations during experiments revealed that, in all cases, breakthrough occurred somewhere on the bottom surface of the soil column and not at the periphery. The time intervals between successive irrigation applications was identical and sufficiently long (1 month) to facilitate the development of cracks.

Table 1 Observed and calculated values of the volume flux density $q(Z, t)$.

Run	1	2	3	4	5	6
Observed parameters:						
q_s (m s^{-1})	4.1×10^{-6}	1.06×10^{-5}	2.2×10^{-5}	2.3×10^{-5}	2.62×10^{-5}	2.80×10^{-5}
t_s (s)	13 900	10 000	4 100	4 500	4 000	3 000
t_{W1} (s)	6 300	3 590	1 536	1 514	1 690	1 056
t_{W2} (s)	6 500	3 800	1 700	1 700	2 200	1 600
Calculated parameters:						
a	5.42	4.06	4.77	4.73	4.38	5.60
b (m s^{-1})	229.79	2.18	4.23	4.54	1.93	42.55
t_W (s)	3 900	1 992	1 525	1 420	1 270	1 209
t_D (s)	14 620	10 490	4 420	4 800	4 290	3 216
$t_D - t_s$ (s)	720	490	320	300	290	216
c_W (m s^{-1})	1.1×10^{-4}	2.16×10^{-4}	2.82×10^{-4}	3.03×10^{-4}	3.38×10^{-4}	3.56×10^{-4}
r^2	0.95	0.95	0.98	0.96	0.97	0.97

q_s is the input rate of the infiltration;
t_s is the duration of infiltration;
t_{W1} is the time at which the first drop of water appeared at the bottom;
t_{W2} is the time at which the entire bottom area is wetted.
a is an exponent, b is the conductance;
t_W is the arrival time of the wetting front;
t_D is the arrival time of the draining front;
c_W is the celerity of the wetting front.

DATA ANALYSIS

Equation (13b) was applied to the decreasing limb of $w(z, t) > t_D$ according to the following procedure. First, the data were transformed into

$$x_i(Z) = \ln\left[\frac{t_D(Z) - t_s}{t - t_s}\right] \tag{17a}$$

$$y_i(Z) = \ln\left[\frac{w_{max} - w_{init}}{w(Z,t) - w_{init}}\right] \tag{17b}$$

The estimation of $t_D(Z)$ followed two steps. The first approximation is due to the inspection of the data graphically (Fig. 2). A series of trial and error estimates, using linear regression as a check on the objective function, equation (22), improved the accuracy. The first regression of

$$y_i = A_1 x_i + B_1 \tag{18}$$

produces $A_1 = 1/(a - 1)$, and thus

$$a = \frac{(a_1 + 1)}{A_1} \tag{19}$$

if $B_1 = 0$. The second linear regression was applied to

$$x_k = w_s\left[\frac{t_D(Z) - t_s}{t_k - t_s}\right]^{1/(a-1)} \tag{20}$$

$$y_k = w(z, t_k) \tag{21}$$

yielding

$$y_k = A_2 x_k + B_2 \tag{22}$$

The procedure involving equations (20)–(22) produces the slope A_2, the intercept B_2, and the coefficient of determination, r^2. The time $t_D(Z)$ in equations (13a)–(20) was optimized such that $A_2 \rightarrow 1$, $B_2 \rightarrow 0$, and $r_2^2 \rightarrow 1$.

The different types of soil moisture were identified at an observation scale defined as the time from the beginning of infiltration, t_0, to the cessation of drainage, t_{end}, (Mdaghri-Alaoui, 1998) (Fig. 2).

The total soil moisture measured from zero is termed θ. Thus:

$\theta(z, t)$: total soil moisture measured at depth z and at time t (variable);

θ_{init}: total soil moisture measured at $t \leq 0$ s (constant);

θ_{max}: maximum soil moisture achieved at the steady state (constant); and

θ_{end}: total soil moisture measured at the end of drainage (constant).

The mobile soil moisture, w, can be defined according to two methods:

(a) mobile soil moisture contributing to total flow:

$$w(z,t) = \theta(z,t) - \theta_{init}\,(\text{variable})$$

$$w_s = \theta_{max} - \theta_{init}\,(\text{constant})$$

(b) mobile soil moisture contributing to rapid flow:

$$w(z,t) = \theta(z,t) - \theta_{end}\,(\text{variable})$$

$$w_s = \theta_{max} - \theta_{end}\,(\text{constant})$$

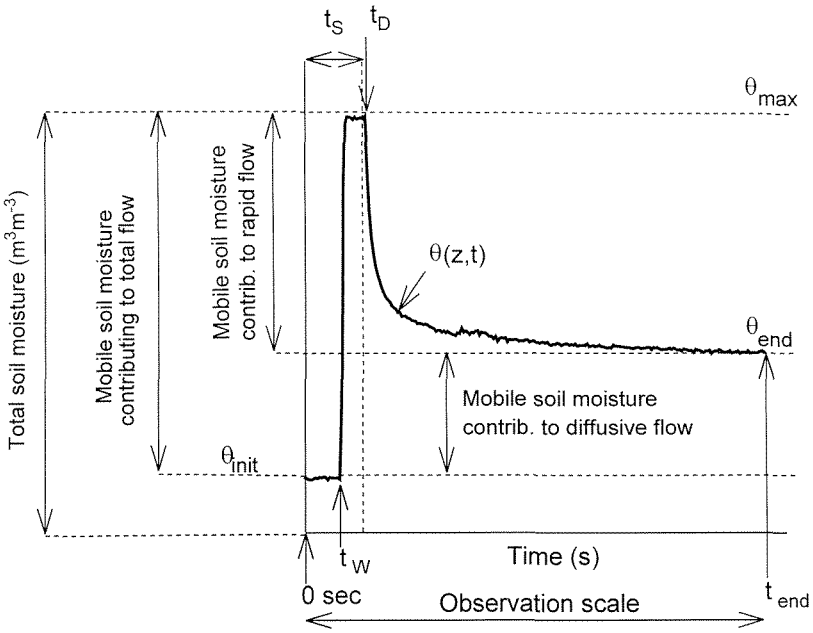

Fig. 2 Evolution of soil moisture and definition of the parameters according to kinematic wave theory (t_s is the duration of infiltration; t_D is the arrival of draining front; $w(z, t)$ is the mobile water content measured at depth z and time t; θ_{max} is the maximum soil moisture measured during infiltration; θ_{init} is the soil moisture prior to infiltration; θ_{end} is the final water content following the passage of the kinematic wave).

Soil moisture is measured in $m^3\ m^{-3}$. The two methods above were used to estimate the kinematic wave parameters.

RESULTS AND DISCUSSION

Analysis of drainage flow

Six infiltration runs of varying intensities were conducted on the soil column (Table 1). Steady state (i.e. $t_W(Z) < t_D(Z) < t_i$) was established for all infiltration runs. Drainage flow, $q(Z, t)$ and model fitting to the observed drainage hydrographs are shown in Figs 3 and 4, respectively.

The parameter b is smaller at intermediate intensities. Its physical interpretation is further investigated. The celerity c_W increased with increasing input rates. The difference $(t_D - t_s)$ decreased with increasing input rates, showing rapid draining of macropores at high rates (quick decrease of outflow $q(Z, t)$). At lower rates, this difference increased (run 1, Fig. 4) and the volume flux density $q(Z, t)$ decreased, indicating the slower drainage of the matrix. Thus, the shape of the draining curve indicates the type of the drainage process. In all cases, the observed flow rates

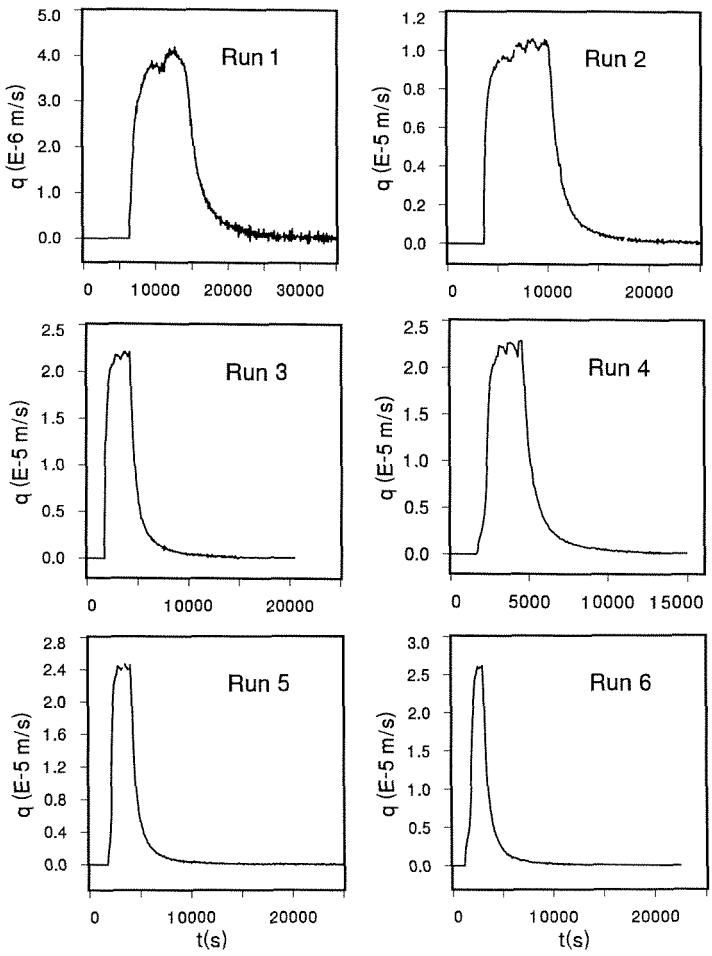

Fig. 3 Experimental hydrographs $q(Z, t)$ observed for all infiltration runs.

dropped dramatically after rainfall ceased, as is characteristic of macropore flow (Thomas & Phillips, 1979), and was essentially zero some hours later (10 h for run 1 and 6 h for run 6).

The modelled arrival time of wetting front at Z, t_W is greater than the observed t_{W1} for runs 1 and 2. For runs 3–6, this parameter is simulated well. At intermediate and high intensities, the beginning of $q(Z, t)$ is well estimated by the kinematic wave approach ($t_{W1} < t_W < t_{W2}$). At lower intensities, the deviation between modelled and observed arrival times is more pronounced. A successful application of the kinematic wave model hinges on the reliable estimation of exponent a.

Di Pietro & LaFolie (1991) conducted successive infiltration runs to characterize water flow through a column consisting of an artificial double-porosity medium. They applied the kinematic wave theory to drainage hydrographs. The range of a was between 4 and 8, and it increased with decreasing volume flux

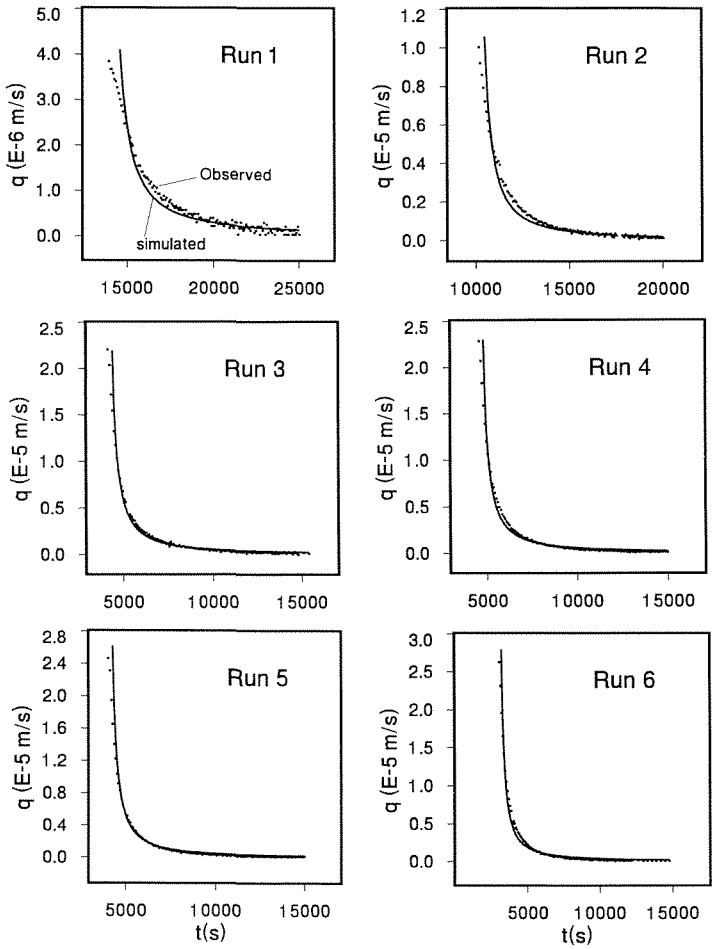

Fig. 4 Fitted and observed drainage hydrographs for all infiltration runs.

density q_s. Exponent a characterizes the flow regime indicating whether water flows dominantly through the matrix or along macropores. The study by Germann & Di Pietro (1996) suggested a equal to 2 for preferential flow along tubes, $a = 3$ for preferential flow along planes and $11 < a < 30$ for diffusive flow (i.e. Richards-type flow), leaving the range of $3 < a < 11$ as a transition between the two types of flow. Our values of a ranged between 4 and 6, the lower values being found at intermediate input intensities (Table 1). For the low and high intensities (run 1 and run 6, respectively) a exceeded 5. At higher intensities, most of the pores contribute to the flux and its spatial distribution is relatively homogeneous. At low input intensities, the propagation of the wetting front is important. At intermediate rates, only some of the coarser pores contribute to most part of the total water flux and the preferential flow predominates. These observations are in agreement with those by Quisenberry *et al.* (1994).

Analysis of soil moisture at three depths

Mobile soil moisture contributing to total flow ($\theta_{max} - \theta_{init}$) Observed and modelled soil moisture $w(z, t)$ at three depths, and the drainage hydrographs are shown in Figs 5 and 6. The observed and calculated parameters resulting from soil moisture simulation at 0.12, 0.26 and 0.33 m are shown in Table 2. The variation of soil moisture at depths of 0.26 and 0.33 m during run 1 show a monotonous increase of soil moisture without rapid decrease shortly after the cessation of infiltration (Fig. 5). This type of reaction indicates a diffusive process which is dominated by capillarity (Mdaghri-Alaoui *et al.*, 1997). Consequently, it was not analysed according to the kinematic wave model (Tables 2 and 3).

At low infiltration rates (run 1), the celerity c_W calculated at 0.12 m depth is lower than that observed in runs 2–6. In all runs, different values of c_W were observed at 0.26 and 0.33 m depths. This observation can be explained by the fact

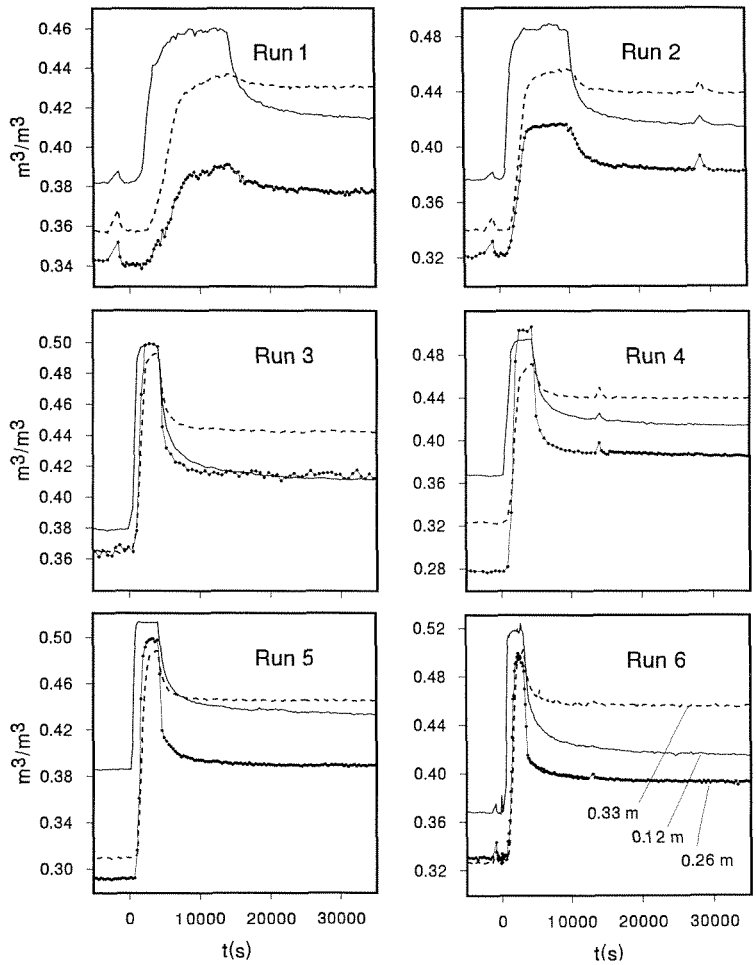

Fig. 5 Soil moisture $w(z, t)$ *vs* time at three depths for all infiltration runs.

that c_W corresponds to the propagation of the wetting front as measured from TDR-moisture readings. Various values of a were obtained. Brooks & Corey (1964) arrived at exponents in the range $3 \leq a \leq 6$. Clapp & Hornberger (1978) found $11 \leq a \leq 26$. The variation of a indicates that the model parameters depend not only on the structure of the porous medium and its moisture but also on the boundary conditions which impact w_s. Exponent a is small if the mobile water is distinguished from the stagnant water. On the contrary, a is large if all soil moisture is considered to participate in the flow process (Tables 2 and 3).

In this study, the exponent a which results from the model application to the TDR data is lower at 0.12 m and varies from 4 to 6. At 0.26 m, it increases slightly and varies between 5 and 9. It increases again at 0.33 m (10–20). This was true for all six infiltration runs, as shown in Table 2. The increase of exponent a with increasing depth suggests that the wetting front increasingly disperses as it progresses

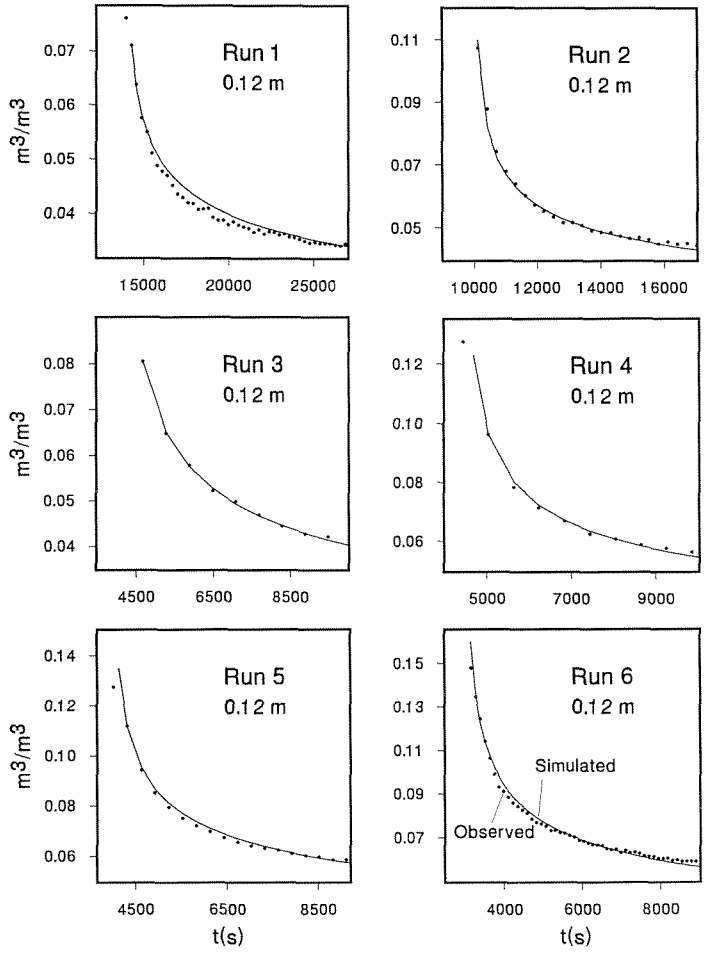

Fig. 6 Fitted and observed values of $w(z, t)$ according to total soil moisture at depth of 0.12 m for all infiltration runs.

Table 2 Observed and calculated values of soil moisture at three depths for the six infiltration runs according to the analysis of total soil moisture.

Run	1	2	3	4	5	6
Observed parameters (depth 0.12 m):						
θ_{max} (m^3 m^{-3})	0.460	0.489	0.500	0.500	0.514	0.520
θ_{init} (m^3 m^{-3})	0.382	0.376	0.380	0.367	0.386	0.367
w_s (m^3 m^{-3})	0.078	0.113	0.120	0.133	0.128	0.153
Calculated parameters (depth 0.12 m):						
a	5.80	5.41	4.35	5.07	5.14	4.50
b (m s^{-1})	17.70	3.33	0.22	0.60	0.62	0.10
t_W (s)	1 409.4	541	661.2	740.2	961.2	823.5
t_D (s)	14 143	10 100	4 252	4 646	4 187	3 183
$t_D - t_s$ (s)	243	100	152	146	187	183
c_W (m s^{-1})	8.5×10^{-5}	2.22×10^{-4}	1.81×10^{-4}	1.63×10^{-4}	1.25×10^{-4}	1.4×10^{-4}
r^2	0.99	0.98	0.99	0.99	0.99	0.99
Observed parameters (depth 0.26 m):						
θ_{max} (m^3 m^{-3})	0.390	0.416	0.500	0.500	0.500	0.500
θ_{init} (m^3 m^{-3})	0.340	0.321	0.368	0.277	0.292	0.333
w_s (m^3 m^{-3})	0.050	0.095	0.132	0.223	0.208	0.167
Calculated parameters (depth 0.26 m):						
a	-	8.06	5.81	9.29	6.94	4.83
b (m s^{-1})	-	4 706.8	17.25	440.9	4.48	0.43
t_W (s)	-	911	256	149	652	570
t_D (s)	-	10 113	4 144	4 516	4 094	3 118
$t_D - t_s$ (s)	-	113	44	16	94	118
c_W (m s^{-1})	-	2.85×10^{-4}	1.0×10^{-3}	1.74×10^{-3}	4.0×10^{-4}	4.53×10^{-4}
r^2	-	0.98	0.98	0.99	0.84	0.89
Observed parameters (depth 0.33 m):						
θ_{max} (m^3 m^{-3})	0.437	0.456	0.494	0.493	0.490	0.500
θ_{init} (m^3 m^{-3})	0.357	0.339	0.366	0.322	0.310	0.333
w_s (m^3 m^{-3})	0.080	0.117	0.128	0.171	0.180	0.167
Calculated parameters (depth 0.33 m):						
a	-	19.74	9.60	13.41	15.41	11.36
b (m s^{-1})	-	$4.3\ 10^{+13}$	$2.07\ 10^{+4}$	$1.7\ 10^{+6}$	$1.3\ 10^{+7}$	$1.6\ 10^{+4}$
t_W (s)	-	2230.6	758.4	630.3	1371.5	2328.8
t_D (s)	-	10113	4179	4547	4089	3205
$t_D - t_s$ (s)	-	113	79	47	89	205
c_W (m s^{-1})	-	$1.48\ 10^{-4}$	$4.34\ 10^{-4}$	$5.15\ 10^{-4}$	$2.41\ 10^{-4}$	$1.4\ 10^{-4}$
r^2	-	0.96	0.96	0.97	0.97	0.96

θ_{max} is the maximum soil moisture measured during the infiltration;
θ_{init} is the soil moisture prior to infiltration.

downward, and drainage is increasingly dominated by flow through a restricting network of macropores.

Mobile soil moisture contributing to rapid flow ($\theta_{max} - \theta_{end}$) Table 3 shows the observed and calculated parameters according to the analysis of mobile soil moisture

Table 3 Observed and calculated values of soil moisture at three depths for the six infiltration runs according to mobile soil moisture.

Run	1	2	3	4	5	6
Observed parameters (depth 0.12 m):						
θ_{max} ($m^3\ m^{-3}$)	0.460	0.489	0.500	0.500	0.514	0.520
θ_{end} ($m^3\ m^{-3}$)	0.410	0.412	0.411	0.411	0.430	0.414
w_s ($m^3\ m^{-3}$)	0.050	0.077	0.089	0.089	0.084	0.106
Calculated parameters (depth 0.12 m):						
a	2.10	1.96	1.84	1.96	2.18	1.85
b ($m\ s^{-1}$)	2.6×10^{-3}	2.12×10^{-3}	1.29×10^{-3}	1.64×10^{-3}	3.21×10^{-3}	1.04×10^{-3}
t_W (s)	1 244	664	712	747	694	775
t_D (s)	14 492	10 339	4 487	4 880	4 318	3 418
$t_D - t_s$ (s)	592	339	387	380	318	418
c_W ($m\ s^{-1}$)	9.65×10^{-5}	1.81×10^{-4}	1.69×10^{-4}	1.61×10^{-4}	1.73×10^{-4}	1.54×10^{-4}
r^2	0.90	0.87	0.86	0.85	0.91	0.88
Observed parameters (depth 0.26 m):						
θ_{max} ($m^3\ m^{-3}$)	0.390	0.416	0.500	0.500	0.500	0.500
θ_{end} ($m^3\ m^{-3}$)	0.370	0.381	0.414	0.384	0.387	0.390
w_s ($m^3\ m^{-3}$)	0.020	0.035	0.086	0.116	0.113	0.110
Calculated parameters (depth 0.26 m):						
a	-	2.06	1.76	2.27	2.26	2.62
b ($m\ s^{-1}$)	-	1.07×10^{-2}	3.50×10^{-3}	1.24×10^{-2}	0.96×10^{-2}	9.78×10^{-2}
t_W (s)	-	851	479	322	423	95
t_D (s)	-	10 412	4 372	4 642	4 187	3 036
$t_D - t_s$ (s)	-	412	272	142	187	36
c_W ($m\ s^{-1}$)	-	3.06×10^{-4}	5.42×10^{-4}	8.04×10^{-4}	6.15×10^{-4}	2.74×10^{-3}
r^2	-	0.86	0.93	0.94	0.97	0.79
Observed parameters (depth 0.33 m):						
θ_{max} ($m^3\ m^{-3}$)	0.437	0.456	0.494	0.493	0.490	0.500
θ_{end} ($m^3\ m^{-3}$)	0.437	0.438	0.442	0.439	0.444	0.454
w_s ($m^3\ m^{-3}$)	0.017	0.018	0.052	0.054	0.046	0.046
Calculated parameters (depth 0.33 m):						
a	-	1.82	1.97	1.90	2.15	2.27
b ($m\ s^{-1}$)	-	1.19×10^{-2}	0.99×10^{-2}	0.92×10^{-2}	2.30×10^{-2}	2.38×10^{-2}
t_W (s)	-	748	587	494	493	693
t_D (s)	-	10 412	4 398	4 760	4 229	3 305
$t_D - t_s$ (s)	-	412	298	260	229	305
c_W ($m\ s^{-1}$)	-	4.42×10^{-4}	5.62×10^{-4}	6.65×10^{-4}	6.67×10^{-4}	4.77×10^{-4}
r^2	-	0.81	0.99	0.86	0.97	0.97

θ_{end} is the final water content following the passage of the kinematic wave.

contributing to rapid flow. The exponent a is very close to 2 in all cases and throughout the soil. This value indicates a rapid flow along macropores as suggested by Germann (1990). It is suggested that exponent a will be constant for all soils if mobile soil moisture can properly be estimated.

Figure 7 shows the relationship between a and the time at which curve fitting stopped, equations (15)–(18). The analysis of mobile soil moisture contributing to

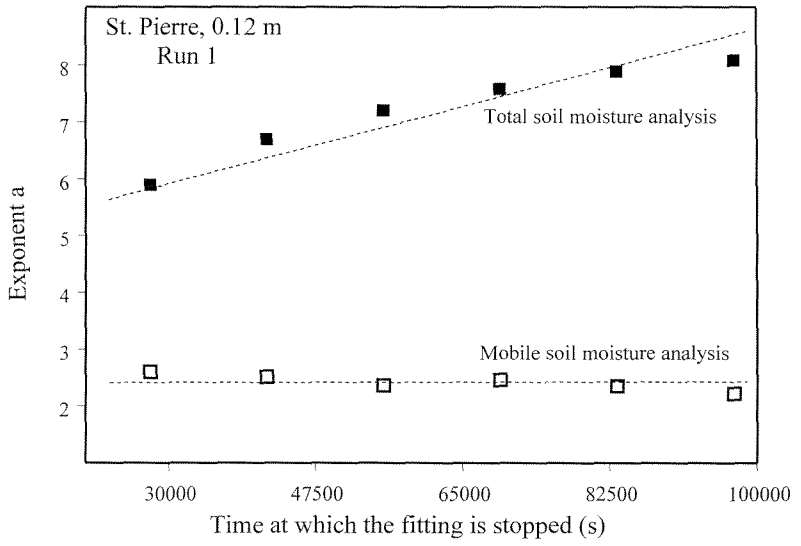

Fig. 7 Sensitivity of exponent *a* with respect to the time interval for each fitted curve.

total flow shows that the exponent *a* increases with increasing time. By contrast, the analysis of mobile soil moisture contributing to rapid flow shows that the exponent *a* is nearly constant and remains close to 2. The observations suggest that the diffusive flow is more pronounced at the end of drainage. The constant value of *a* estimated from mobile soil moisture contributing to rapid flow indicates that the macropores carried water during drainage.

The values of *a* obtained from the model application to water outflow are in the range of 4.06–5.60. These values are comparable to those obtained from the model application to TDR data at 0.12 m (values ranged between 4.35 and 5.80). Moreover, the increasing values of *a* (resulting from the analysis of mobile soil moisture contributing to total flow) with depth indicates that the wetting front dispersion increases with depth. These observations suggest that the saturation conditions at the surface cause a shock wave which propagates deeper into the soil along macropores. By contrast, the dispersion of the wetting front in the matrix is due to preferential flow which causes the heterogeneity in the soil moisture.

Water balance

The volume of water flowing through macropores, $V(Z)$, has been calculated through application of the kinematic wave theory. In seven out of sixteen cases, the calculated volume is overestimated, exceeding the irrigation volume input (Table 4).

Reasonable simulations of the volume of water flowing through macropores were observed at a depth of 0.12 m whilst discrepancies arose at depths of 0.26 and 0.33 m. The latter may be explained by the following (Mdaghri-Alaoui, 1998):

(a) the estimation of mobile water content contributing to rapid flow is based on

Table 4 Evolution of the graph $w(z, t)$ and definition of the parameters related to the kinematic wave theory (see text for explanation).

Run	1	2	3	4	5	6
V_0 (infiltrated)	57	106	90.2	103.5	105	84
$V_{0.12}$	67	139	62	64	58	49
$V_{0.12}/V_0$	1.18	1.31	0.69	0.62	0.55	0.58
$V_{0.26}$	-	107	191	420	278	903
$V_{0.26}/V_0$	-	1.01	2.12	4.06	2.65	10.75
$V_{0.33}$	-	79	120	162	123	66
$V_{0.33}/V_0$	-	0.75	1.33	1.56	1.17	0.79

$V_{0.12}$, $V_{0.26}$ and $V_{0.33}$ are the values of calculated volume at depths of 0.12, 0.26 and 0.33 m respectively;
St Peters Insel soil, mobile soil moisture contributing to rapid flow.

simple linear separation—it could be obtained dynamically;

(b) the dispersion of the wetting front with depth (according to the analysis of mobile soil moisture contributing to total flow) shows that the kinematic wave theory was not validated successfully at depths of 0.26 and 0.33 m;

(c) the estimation of $V(Z)$ depends on the parameter b which is sensitive to the analysis procedures.

The method of separation of the two types of soil moisture used here is promising and permits the application of the kinematic wave theory to soil moisture variations. The discrepancies in water balance suggest that this separation could be improved by introducing dynamic processes.

CONCLUSIONS

The kinematic wave model has the advantage of simplicity. Measured drainage and soil moisture variations were reasonably well simulated by the kinematic wave approach. The shape of the draining curve, expressed with exponent a, indicates the type of the drainage process. The applicability of the model to both drainage flow and moisture variations suggests that the exponent a indicates which flow type dominates: matrix or macropore flow. The parameter a is observed to vary with variation of infiltration intensity. According to the observations, preferential flow takes place at intermediate infiltration rates. The analysis of mobile soil moisture contributing to total flow indicates that the exponent a increases with increasing depth suggesting an increase of the wetting front dispersion with progressive depth. The exponent a, resulting from the interpretation of mobile soil moisture contributing to rapid flow, is close to 2 throughout the soil. This value indicates flow along macropores and constitutes a positive validation of the model. Dispersion of the wetting front increased with decreasing input intensities. The simple method used to separate the two types of soil moisture contributing to rapid and diffusive flow is promising but not sufficient to reproduce the volume of water flowing in macropores from the simple measurements of water content by TDR-probes. To predict water outflow from the application of the simple kinematic wave model further investi-